Available online at www.sciencedirect.com

ScienceDirect

Scripta Materialia 70 (2014) 59–62

Scripta MATERIALIA

www.elsevier.com/locate/scriptamat

Grain boundary films in Al–Zn alloys after high pressure torsion

B.B. Straumal,[a,b,c,d,*] X. Sauvage,[e] B. Baretzky,[b] A.A. Mazilkin[a,b] and R.Z. Valiev[f]

[a] *Institute of Solid State Physics, Russian Academy of Sciences, Chernogolovka, Moscow 142432, Russia*

[b] *Karlsruher Institut für Technologie, Institut für Nanotechnologie, Hermann-von-Helmholtz-Platz 1, 76344 Eggenstein-Leopoldshafen, Germany*

[c] *Moscow Institute of Physics and Technology (State University), Institutskii Per. 9, 141700 Dolgoprudny, Russia*

[d] *Laboratory of Hybrid Nanomaterials, National University of Science and Technology "MISIS", Leninskii Prospekt 4, 119049 Moscow, Russia*

[e] *Groupe de Physique des Matériaux, Université de Rouen, CNRS, UMR 6634, Avenue de l'Université, BP 12, 76801 St-Etienne-du-Rouvray, France*

[f] *Institute of Physics of Advanced Materials, Ufa State Aviation Technical University, 12 Karl Marx Str., Ufa 450000, Russia*

Received 15 August 2013; revised 17 September 2013; accepted 18 September 2013
Available online 25 September 2013

In ultra-fine grained Al–Zn alloys after high pressure torsion Al/Al grain boundaries (GBs) completely, partially or pseudopartially wetted by Zn in the solid state have been observed using analytical and high resolution electron microscopy. In the latter case the solid Zn particles in the triple joints form a non-zero contact angle $\theta = 80$–$160°$ with Al/Al GBs. Simultaneously, a 2–10 nm thick uniform Zn-rich layer is present in the Al/Al GBs.

Keywords: Severe plastic deformation; High pressure torsion; Grain boundaries; Wetting; Phase transformations

During severe plastic deformation (SPD) a steady state is usually reached after a certain strain. The grain size, strength, hardness, hydrogen content, long-range order parameter, composition of phases, etc. stop evolving with increasing strain (i.e. the number of equal-channel angular pressing passes, rotation angle during high-pressure torsion (HPT), or number of accumulative roll bonding passes) [1–3]. Moreover, the structure and composition of phases in the steady state usually differ from those before SPD [4,5]. After SPD phases were frequently found which could also appear after long annealing at a certain temperature T_{eff} [6–13]. One would expect that SPD can force not only bulk but also grain boundary (GB) phase transformations. The phenomenon of GB wetting is known to be very sensitive to the temperature, pressure and composition of phases [14–16]. Usually partial wetting (PW) and complete wetting (CW) of surfaces or interfaces can be distinguished. If a liquid droplet partially wets a solid surface (Fig. 1a) then $\sigma_{sg} - \sigma_{sl} = \sigma_{lg}\cos\theta$, where σ_{sg} is the free energy of the solid/gas interface, σ_{sl} is the free energy of the solid/liquid interface, σ_{lg} is that of the liquid/gas interface and θ is the contact angle. If a liquid droplet partially wets the boundary between two solid grains (Fig. 1b) then $\sigma_{gb} = 2\sigma_{sl}\cos\theta$, where σ_{gb} is the free energy of a GB. Any free surface or GB which is not covered by the liquid droplet remains dry and contains only the adsorbed atoms with a coverage below one monolayer. In the case of complete wetting (Fig. 1c and d) $\sigma_{sg} > \sigma_{lg} + \sigma_{sl}$ or $\sigma_{gb} > 2\,\sigma_{sl}$ the contact angle is zero, and liquid spreads over the free surface or

* Corresponding author at: Institute of Solid State Physics, Russian Academy of Sciences, Chernogolovka, Moscow 142432, Russia. Tel.: +7 916 6768673; fax: +7 499 2382326; e-mail: straumal@issp.ac.ru

1359-6462/$ - see front matter
http://dx.doi.org/10.1016/j.scriptamat.2013.09.019

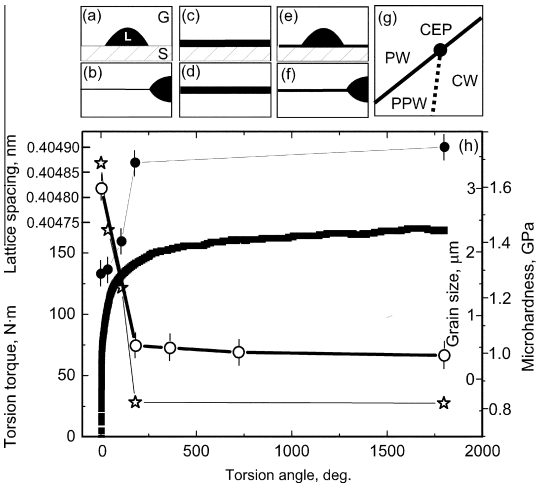

Figure 1. Schemes for the wetting of free surfaces and GBs. (a) Partial surface wetting; (b) partial GB wetting; (c) complete surface wetting; (d) complete GB wetting; (e) pseudopartial surface wetting; (f) pseudopartial GB wetting; (g) generic wetting phase diagram [33]. L, liquid phase; S, solid phase; G, gas phase; PW, partial wetting; CW, complete wetting; PPW, pseudopartial wetting; CEP, critical end point. Thick lines mark the discontinuous (first order) wetting transition, thin lines mark the continuous (second order) wetting transition. (h) Dependence of torsion torque (filled squares), lattice spacing (filled circles [5]), microhardness (open stars [5]) and grain size (open circles) on the HPT rotation angle (strain) for the Al–30 wt.% Zn alloy. The lines are guides for the eye. The values at zero rotation angle were measured after applying a pressure of 5 GPa, but without torsion.

between grains. The PW ↔ CW transition can proceed by the changing temperature and/or pressure [14–17].

The Al–Zn system is a good candidate for the investigation of GB wetting under SPD [2,7,8,18–20]. Various GB wetting transitions proceed in Al–Zn in equilibrium. In (Al) + L and (Zn) + L two phase areas of the Al–Zn phase diagram the transition from partial to complete wetting of (Al)/(Al) GBs and (Zn)/(Zn) GBs by the liquid phase occurs [18]. ((Al) and (Zn) are solid solutions based on Al and Zn.) The wetting phase can also be solid. In the (Zn) + (Al) area the (Zn)/(Zn) GBs can be either partially or completely wetted by a layer of a second solid phase (Al) [19]. Below 205 °C the first (Al)/(Al) GBs completely wetted by solid (Zn) layers appear [20]. HPT of as-cast Al–Zn alloys leads to extremely rapid decomposition of supersaturated Al–Zn solid solutions and almost pure Al and Zn grains appeared instead [2,7]. Al–Zn alloys after HPT have ultra-fine grains and possess extremely high ductility [21,22]. This permits us to suppose that a soft lubricating layer exists along (Al)/(Al) GBs which facilitates GB sliding.

We performed HPT (5 GPa, 300 K, 5 rotations, 1 rpm) of Al-30 wt.% Zn polycrystals made of high purity components. Analytical transmission electron microscopy (TEM) has been performed with a probe-corrected ARM200F JEOL microscope operated at 200 kV. High angle annular dark field (HAADF) images were recorded in scanning mode (STEM) using a probe size of 0.2 nm with a convergence angle of 34 mrad and collection angles in the range 80–300 mrad. To quantify the local Zn concentration energy-dispersive X-ray spectroscopy (EDS) was performed using a JEOL JED2300 detector. Similarly to Mazilkin et al. [2] and Straumal [7], the supersaturated (Al) solid solution almost completely decomposed. The mean Al grain size decreased from 500 μm before deformation to 400 nm after HPT (Fig. 1h).

Figure 1h shows the dependence of torsion torque (filled squares) on the rotation angle (strain) for the Al–30 wt.% Zn alloy. After short work hardening during the first rotation of the anvils the torsion torque reaches a steady state and remains constant. The microhardness (open stars [2]), lattice spacing (filled circles [2]) and grain size (open circles) reach a steady state almost simultaneously with the torsion torque. The micrograph in Figure 2 (right inset) shows a HAADF STEM image where the contrast is related to the local average atomic number (Z-contrast). Thus Zn-rich zones appear bright, while darker areas correspond to Al. The GB between grains 3 and 4 is completely wetted by the solid (Zn) phase and contains a rather thick uniform Zn-rich layer. The plot of the HAADF signal across GB 3/4 (left inset in Fig. 2) has a strong peak with a width of 22 nm. Other (Al)/(Al) GBs in the micrograph are partially wetted. The chain of lenticular (Zn) particles with a non-zero contact angle is visible in the GB between grains 4 and 6. The plots of the HAADF signal across the partially wetted GBs reveal no peaks. In other words, these GBs between (Zn) particles remain completely "dry".

GBs completely and partially wetted by a second solid phase have been observed previously after long annealing in Al–Zn alloys [19,20] and in other systems like Al–Mg [23] or Cu–Co [24]. However, the HPT-treated Al–Zn alloys also contain something unusual, namely (Al)/(Al) GBs with a thin uniform Zn-enriched layer in contact with Zn grains and having a non-zero contact angle. Such a case is shown in Figure 3. The contact area of a Zn grain (left bottom corner) and an (Al)/(Al) GB (aligned from left bottom to right top) is clearly shown (Fig. 3a). The contact angle of the Zn grain

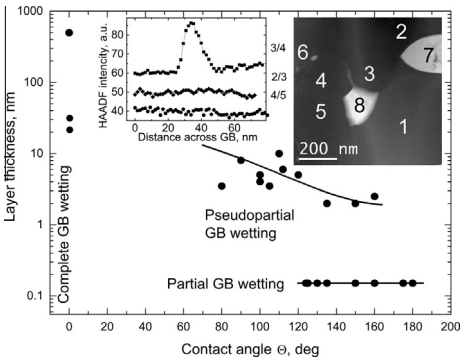

Figure 2. Correlation between the observed thickness of the Zn-rich layer in (Al)/(Al) GBs and the contact angle between Zn particles in the (Al)/(Al) GB triple joints and the respective (Al)/(Al) GBs. Three areas are visible: (1) completely wetted GBs with $\theta = 0°$ and a thick GB layer; (2) partially wetted GBs with $\theta = 120°$ and 180° without a Zn-rich layer; (3) pseudopartially wetted GBs with $\theta = 80–160°$ and thin (2–10 nm) Zn-rich layers. (Right inset) A Z-contrast image obtained by HAADF STEM showing two bright (Zn) grains and six dark (Al) grains. The complete GB wetting layer is visible in the 3/4 GB. A chain of small lenticular (Zn) grains is visible in the 4/6 GB. (Left inset) The HAADF signal intensity across the 2/3, 3/4 and 4/5 (Al)/(Al) GBs.

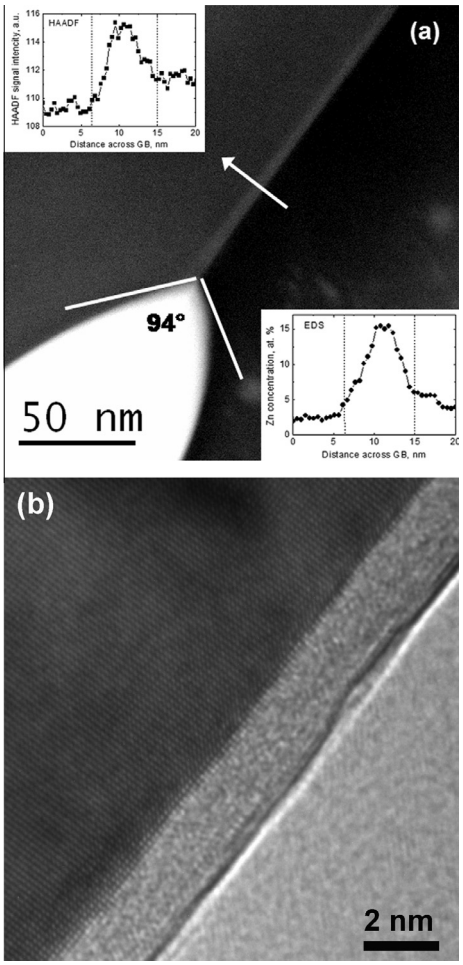

Figure 3. (a) Z-contrast image obtained by HAADF STEM showing a Zn grain (bright) in the bottom left corner and an (Al)/(Al) grain boundary (aligned from left bottom to right top) wetted by a uniform Zn-rich layer in the Al–30 wt.% Zn alloy after HPT (5 GPa, 5 rotations, 1 rpm). The contact angle of the Zn grain with the (Al)/(Al) GB is 94°. (Left inset) HAADF signal intensity across the (Al)/(Al) GB showing that the apparent thickness of the Zn-rich layer is about 8 nm (the arrow in (a) indicates the location of the profile). (Right inset) Zn concentration gradient across the (Al)/(Al) GB at the same place, estimated by EDS. (b) HRTEM image showing a featureless wetting layer along an (Al)/(Al) GB.

with the (Al)/(Al) GB is about 94°. The GB clearly appears on the image as a bright line, indicating local Zn enrichment. This feature was confirmed by the EDS line scan analysis performed across the boundary (Fig. 3a, right inset). The maximum Zn concentration along the boundary was 15 ± 0.5 at.%, and large gradients are present (over 4 nm on each side of the interface, also confirmed by the plot of the HAADF signal across the GB in Fig. 3a, left inset). Part of this gradient might be attributed to a misalignment of the GB under the electron beam. However, one should note that a 2 nm wide plateau can be clearly seen on the profile, indicating that the GB is not completely wetted by a pure Zn layer. Moreover, the thickness of the Zn-rich GB layer is very uniform along all visible GBs. The micrograph obtained by high resolution TEM (Fig. 3b) shows an intermediate layer between Al grains at higher magnification. Its thickness is about 2 nm. If one analyses numerous GBs after HPT one can observe, in contrast to the long annealed samples [20], not only (Al)/(Al) GBs completely and partially wetted by the solid Zn phase, but also numerous GBs with $\theta > 0$ and a thin Zn-enriched layer (Fig. 2). The contact angles for these GBs vary between $\theta = 80°$ and 160° and TEM data show that they are not symmetrical. The increase in θ from 80° and 160° correlates with a decrease in thickness of the Zn-enriched GB layer from 10 to 2 nm. The PW GBs do not have any visible Zn enrichment and have contact angles between $\theta = 120°$ and 180°.

What is the physical reason for this phenomenon? In the case of partial wetting, when $\theta > 0°$, the neighboring GB should be "dry" (Fig. 2). A thin enriched GB layer can exist in the case of complete wetting and $\theta = 0°$, if the amount of liquid is small and the surface (or GB) area is large. In this case the liquid spreads until two solid grains or a solid and gas begin to interact with each other through the liquid layer. The liquid forms a kind of "pancake" with a thickness e_s of about 2–5 nm [25,26]. The GB prewetting layers (or complexions) have a similar appearance (i.e. mostly amorphous and uniformly thin) if the bulk wetting phase is absent [17,27–32]. However, in our samples a second wetting phase is present in large amounts. It has been theoretically predicted that in some cases a state of so-called pseudopartial wetting (PPW) occurs between PW and CW [26]. In this case for a contact angle $\theta > 0°$ the liquid droplet does not spread over the substrate, but a thin (a few nanometres) precursor film exists around the droplet and separates the substrate and gas (Fig. 1e). In the case of PPW the precursor exists together with liquid droplets, and in the case of complete wetting the droplets disappear, forming a "pancake". The generic phase diagram (Fig. 1g) [33] shows that a line of discontinuous PW ↔ CW transformations should divide in the critical end point (CEP) into discontinuous PW ↔ PPW and continuous PPW ↔ CW lines.

A sequence of discontinuous PW ↔ PPW and continuous PPW ↔ CW transformations was observed for the first time in an alkane/water mixture [31]. The CEP was observed in a mixture of pentane and hexane which was deposited on an aqueous solution of glucose [33]. The first direct measurement of the contact angle in the intermediate wetting state (PPW) was performed in the sequential wetting of hexane on salt brine [33]. Later the formation of Pb, Bi and binary Pb–Bi precursors surrounding liquid or solidified droplets was observed on the surface of solid copper [35]. PPW should in principle also exist at GBs (Fig. 1f). Intergranular films (IGFs) with a uniform thickness of few nanometres have frequently been observed in GBs [28,29]. In most cases they form a zero contact angle with a small amount of bulk liquid phase remaining in GB triple junctions [36]. This case corresponds to complete GB wetting and a deficit of bulk liquid. If the amount of bulk liquid phase in GB triple junctions is low and the solid/liquid interface is concave it is not easy to prove whether $\theta = 0°$ or $\theta > 0°$. The case of pseudopartial GB wetting can be clearly identified only if $\theta > 60°$ and the solid/liquid interface is convex [36].

Figure 3 gives us direct evidence that that a few nanometer thick uniform Zn-rich "precursor" layer can exist in (Al)/(Al) GBs, together with a non-zero contact angle between Zn grains and (Al)/(Al) GBs. This is consistent with the properties one would expect from a PPW precursor [33–35]. This is direct and unequivocal evidence for PPW of (Al)/(Al) GBs. According to the generic wetting phase diagram (Fig. 1g) [33] the line of PW ↔ CW discontinuous transitions separates at the CEP into a line of PW ↔ PPW discontinuous transitions and a line of PPW ↔ CW continuous transitions. In the Al–Zn system both discontinuous and continuous GB wetting transitions by the liquid phase were observed [18]. The second solid phase can also wet both (Al)/(Al) and (Zn)/Zn) GBs [19,20]. Therefore, it is no surprise to find GBs which are pseudopartially wetted by a second solid phase in these alloys. However, instead of long anneals we exploited steady state obtained by HPT.

Thus the experimental evidence is found that PPW (1) occurs not only on surfaces but at solid/solid interfaces (grain boundaries) and (2) the second (wetting) phase is not liquid but solid. This phenomenon takes place in the Al–Zn system, where a discontinuous GB wetting transition occurs in the (Al) + L two phase area of the phase diagram, changing to a continuous transition in the (Zn) + L area. PPW was not observed after conventional annealing and subsequent quenching, but after HPT in the steady-state stage. PPW of Zn-enriched GB films can explain the unusual superductility of ultrafine grained Al–Zn alloys after HPT.

The work was partially supported by the Russian Foundation for Basic Research (Grants nos. 11-03-01198 and 13-08-90422), the Russian Federal Ministry for Education and Science (Grant 14.A12.31.0001), the EraNet. Rus programme (Grant STProjects-219) and the Karlsruhe Nano Micro Facility.

[1] R.Z. Valiev, R.K. Islamgaliev, I.V. Alexandrov, Progr. Mater. Sci. 45 (2000) 103.
[2] A.A. Mazilkin, B.B. Straumal, M.V. Borodachenkova, et al., Mater. Lett. 84 (2012) 63.
[3] V.V. Stolyarov, R. Lapovok, I.G. Brodova, et al., Mater. Sci. Eng., A 357 (2003) 159.
[4] X. Sauvage, A. Chbihi, X. Quelennec, J. Phys. 240 (2010) 012003.
[5] B.B. Straumal, A.A. Mazilkin, B. Baretzky, et al., Mater. Trans. 53 (2012) 63.
[6] X. Sauvage, P. Jessner, F. Vurpillot, et al., Scripta Mater. 58 (2008) 1125.
[7] B.B. Straumal, B. Baretzky, A.A. Mazilkin, et al., Acta Mater. 52 (2004) 4469.
[8] A.A. Mazilkin, B.B. Straumal, E. Rabkin, et al., Acta Mater. 54 (2006) 3933.
[9] X. Sauvage, Y. Ivanisenko, J. Mater. Sci. 42 (2007) 1615.
[10] X. Sauvage, L. Renaud, B. Deconihout, et al., Acta Mater. 49 (2001) 389.
[11] B.B. Straumal, A.A. Mazilkin, S.G. Protasova, et al., Mater. Sci. Eng., A 503 (2009) 185.
[12] Yu. Ivanisenko, I. MacLaren, X. Sauvage, et al., Acta Mater. 54 (2006) 1659.
[13] M.T. Pérez-Prado, A.P. Zhilyaev, Phys. Rev. Lett. 102 (2009) 175504.
[14] B.B. Straumal, W. Gust, T. Watanabe, Mater. Sci. Forum 294 (296) (1999) 411.
[15] B. Straumal, W. Gust, D. Molodov, Interface Sci. 3 (1995) 127.
[16] B. Straumal, E. Rabkin, W. Lojkowski, et al., Acta Mater. 45 (1997) 1931.
[17] W.D. Kaplan, D. Chatain, P. Wynblatt, et al. J. Mater. Sci. 48 (2013) 5681.
[18] B.B. Straumal, A.S. Gornakova, O.A. Kogtenkova, et al., Phys. Rev. B 78 (2008) 054202.
[19] G.A. López, E.J. Mittemeijer, B.B. Straumal, Acta Mater. 52 (2004) 4537.
[20] S.G. Protasova, O.A. Kogtenkova, B.B. Straumal, et al., J. Mater. Sci. 46 (2011) 4349.
[21] R.Z. Valiev, M.Y. Murashkin, A. Kilmametov, et al., J. Mater. Sci. 45 (2010) 4718.
[22] N.Q. Chinh, T. Csanádi, T. Győri, et al., Mater. Sci. Eng., A 543 (2012) 117.
[23] B. Straumal, R. Valiev, O. Kogtenkova, et al., Acta Mater. 56 (2008) 6123.
[24] B.B. Straumal, O.A. Kogtenkova, A.B. Straumal, et al., J. Mater. Sci. 45 (2010) 4271.
[25] J. Luo, Crit. Rev. Solid State Mater. Sci. 32 (2007) 67.
[26] F. Brochard-Wyart, J.M. di Meglio, D. Quéré, et al., Langmuir 7 (1991) 335.
[27] B.B. Straumal, A.A. Mazilkin, O.A. Kogtenkova, et al., Philos. Mag. Lett. 87 (2007) 423.
[28] D. Bonn, J. Eggers, J. Indekeu, et al., Rev. Mod. Phys. 81 (2009) 739.
[29] J. Luo, Y.-M. Chiang, J. Am. Ceram. Soc. 82 (1999) 916.
[30] L.-S. Chang, E. Rabkin, B.B. Straumal, et al., Defects Differ. Forum 156 (1998) 135.
[31] J. Schölhammer, B. Baretzky, W. Gust, et al., Interf. Sci. 9 (2001) 43.
[32] E.I. Rabkin, L.S. Shvindlerman, B.B. Straumal, Int. J. Mod. Phys. B 5 (1991) 2989.
[33] S. Rafaï, D. Bonn, E. Bertrand, et al., Phys. Rev. Lett. 92 (2004) 245701.
[34] E. Bertrand, H. Dobbs, D. Broseta, et al., Phys. Rev. Lett. 85 (2000) 1282.
[35] J. Moon, S. Garoff, P. Wynblatt, et al., Langmuir 20 (2004) 402.
[36] B.B. Straumal, A.O. Rodin, A.E. Shotanov, et al., Defects Diffus. Forum 333 (2013) 175.